ELSEVIER

NeuroImage

www.elsevier.com/locate/ynimg
NeuroImage 42 (2008) 49–59

Dynamics of oxygen delivery and consumption during evoked neural stimulation using a compartment model and CBF and tissue P_{O2} measurements

Alberto L. Vazquez,[a,*] Kazuto Masamoto,[b] and Seong-Gi Kim[a]

[a]*Department of Radiology, University of Pittsburgh, Pittsburgh, PA, USA*
[b]*Molecular Imaging Center, National Institute of Radiological Sciences, Chiba, Japan*

Received 8 December 2007; revised 7 March 2008; accepted 5 April 2008
Available online 16 April 2008

The dynamics of blood oxygen delivery and tissue consumption produced by evoked stimulation of the rat somato-sensory cortex were investigated. Tissue oxygen tension (P_{O2}) and laser Doppler flowmetry (LDF) measurements were recorded under two experimental conditions: normal, which represented both oxygen delivery and consumption, and suppressed CBF (achieved using a vasodilator), which only represented tissue oxygen consumption. Forepaw stimulation for 10 s produced increases of 27.7% and 48.8% in tissue P_{O2} and LDF signal under normal conditions, respectively. The tissue P_{O2} response peaked 9.8 s after stimulation onset and did not show any early transient decreases indicating that measurable oxygen deficits are not required to increase the delivery of oxygen by blood flow. Under suppressed CBF conditions, the LDF signal was mostly suppressed while the tissue P_{O2} decreased by 11.7% and reached a minimum 10.8 s after stimulation onset. These data were analyzed using a dynamic model that described the transport of oxygen from blood to tissue. In order to explain the differences between the model prediction of the tissue P_{O2} changes and the experimental data, several hypothetical scenarios were considered, such as changes in the vascular volume, permeability–surface area or arterial oxygenation. The increase in tissue P_{O2} was found to probably require the recruitment of upstream oxygen from larger arteries as well as increases in the vascular volume at the oxygen exchange sites. The amplitude of the estimated tissue tension of oxygen delivered was about 2.7x larger than the estimated consumption under normal conditions (45.7% vs. 17.1%, respectively).

Keywords: CBF; CMRO2; Oxygen Delivery; Brain; Oxygen transport; Microcirculation; fMRI

Introduction

Brain function relies on the delivery of oxygen from blood for its metabolism in tissue. Under normal resting physiologic conditions, arterial blood carries sufficient oxygen to satisfy the demand of tissue while also maintaining a relatively high venous blood oxygenation. Moreover, during evoked neural activity both the cerebral blood flow (CBF) and the cerebral metabolic rate of oxygen (CMR_{O2}) increase (Fox et al., 1988; Davis et al., 1998; Kim et al., 1999; Shulman et al., 2001). It has also been observed that the suppression of the stimulation-evoked CBF response achieved using a vasodilator does not alter cortical electrical activity and that the decrease in tissue oxygen tension due to the metabolic increase does not decrease below hypoxic levels (Fukuda et al., 2006; Masamoto et al., 2007, 2008). Therefore, the increase in CBF appears to be unnecessary because, not only does it exceed the demand of tissue (Weiss et al., 1983), the baseline supply of oxygen in blood is sufficient to satisfy the functional demands of tissue. Therefore, the role of the evoked hemodynamic response due to changes in function has not been clearly understood. It is possible that a dynamic mismatch between blood oxygen delivery and tissue oxygen consumption plays an important role, but these temporal changes have yet to be carefully investigated. In particular, investigating the properties of oxygen supply is not trivial since it is difficult to generate sudden changes in blood flow alone without changes in oxygen consumption. Any information on the properties of these processes may help understand the dynamic role of oxygen delivery and consumption in functional neurophysiology.

Oxygen sensors have been reliably used to measure the absolute concentration of dissolved oxygen in living tissues, including the brain, and blood vessels (Vovenko 1999; Ances et al., 2001; Thompson et al., 2003; Masamoto et al., 2003). Oxygen sensors are generally sensitive to a volume that spans about 10 times the electrode diameter (Fatt, 1976). Additionally, these sensors can have sufficient temporal sensitivity to detect transient decreases in signal due to oxygen consumption and also transient increases in signal due to an increased delivery of oxygen by increases in blood flow (Masamoto et al., 2003). The changes in CBF can be measured using numerous techniques,

* Corresponding author.
E-mail address: alv15@pitt.edu (A.L. Vazquez).
Available online on ScienceDirect (www.sciencedirect.com).

1053-8119/$ - see front matter © 2008 Elsevier Inc. All rights reserved.
doi:10.1016/j.neuroimage.2008.04.024

including laser Doppler flowmetry (LDF). This technique relies on the scatter of light by moving cells in blood that generates a Doppler shift that is indicative of the blood flow. LDF has a sub-millimeter spatial sensitivity and fast temporal sensitivity (Arbit and DiResta, 1996), and can be easily incorporated with oxygen sensor measurements.

The objective of this work was to investigate the dynamics of the blood oxygen delivery and its consumption in tissue produced by the evoked changes in CBF and tissue CMR_{O2} due to the stimulation of the rat somato-sensory cortex. For this purpose, two conditions (control and suppressed CBF) were established in all the animals tested whereby LDF and tissue oxygen tension (P_{O2}) signals were measured. These data were analyzed using a model that described the transport of oxygen from blood to tissue. The tissue P_{O2} data obtained under control conditions (also referred to as normal conditions) was used to represent both oxygen delivery and consumption, while the tissue P_{O2} data under suppressed CBF conditions was used to determine the tissue oxygen consumption. The changes in oxygen delivery were inferred from the changes in CBF and tissue P_{O2} under control conditions considering the tissue oxygen consumption determined from the suppressed CBF condition data. The following specific questions were investigated using these data and the oxygen transport model: (1) How does the delivery of oxygen change due to the evoked hemodynamic response in order to satisfy the changes in tissue oxygen represented in the data? (2) What are the possible mechanisms responsible for the changes in blood oxygen delivery? The results provided by the model were investigated over physiological ranges for the arterial oxygen concentration and tissue oxygen consumption rate as well as other model parameters. The validity of the assumptions made was also investigated and a preliminary model that describes the behavior observed in the data is proposed.

Methods

Experimental design and data collection

The data used in this work was obtained by our group and is described in detail in the following reference (Masamoto et al., 2007, 2008). A summary of the important details regarding the animal preparation, experimental details and data collection follows.

Five male Sprague–Dawley rats (400 to 560 g) were used under an experimental protocol approved by the University of Pittsburgh Institutional Animal Care and Use Committee. The animals were initially anesthetized using isoflurane (5%), nitrous oxide (50 to 65%) and oxygen (30 to 50%) for intubation and placement of catheters in the femoral artery and femoral vein. The respiration rate and volume were controlled using a ventilator. After intubation, the animals were placed in a stereotaxic frame and the skull was exposed and thinned over the somato-sensory area. The anesthesia and breathing mixture were then changed to isoflurane (1.5%), oxygen (25 to 30%) and air (70 to 75%). The arterial blood pressure, respiration rate, heart rate, rectal temperature, expired CO_2 tension and isoflurane level were monitored and recorded using a polygraph data acquisition software.

Two needle electrodes were placed in the right forepaw of the animals for electrical stimulation. A short stimulation experiment was performed to locate the activation area using optical imaging (Masamoto et al., 2007, 2008). A small hole was then made over the activation area and the oxygen sensor was placed 0.3 mm under the cortical surface to record tissue P_{O2}. The LDF probe was also placed over the activation area just over the thin skull preparation and less than 0.5 mm from the oxygen sensor location. The LDF sensitivity area spanned about 450 μm while the tissue P_{O2} sensitivity spanned at most 300 μm. Evoked stimulation of the somato-sensory cortex was then performed while recording LDF and P_{O2} under two different conditions. The stimulation consisted of 60 electrical stimulation pulses (1.2 mA and 1.0 ms in duration) delivered at a frequency of 6 Hz every 80 s for 1210 s. These stimulation parameters were previously optimized for isoflurane anesthesia (Masamoto et al., 2007).

Experimental conditions

Two experimental conditions were used: a control condition and a suppressed CBF condition. The control condition was the default condition established as described above. The changes in tissue P_{O2} measured during this condition result from both oxygen delivery (i.e. the oxygen supplied by the blood as a function of the CBF response) and oxygen consumption (i.e. the oxygen metabolism in brain tissue). The suppressed CBF condition required the administration of the vasodilatory agent, sodium nitroprusside (sNP). This agent dilates blood vessels and as a result suppresses the CBF response during evoked stimulation without altering neural activity (Nagaoka et al., 2006; Fukuda et al., 2006). The infusion of the agent was adjusted to maintain a mean arterial blood pressure between 40 and 45 mmHg over the course of the evoked stimulation experiment. The infusion of the agent was terminated after approximately 25 min and all the animals were re-tested after the control condition was re-established (after about 1 h) to verify the functional response was the same as that prior to sNP administration. The neural response was also verified to be the similar between control and sNP conditions using a platinum electrode embedded in the oxygen sensor (Masamoto et al., 2007, 2008). In the suppressed CBF condition, the changes tissue P_{O2} are mostly due to oxygen consumption.

Oxygen exchange model

An overview of the model used to describe the dynamics of the transport of oxygen from blood to tissue with evoked neural stimulation follows. For a detailed description of the model please refer to (Valabregue et al., 2003). Two compartments were considered: a capillary blood compartment and a tissue compartment. The capillary compartment consisted of a homogenous suspension of blood where oxygen is bound to hemoglobin and also dissolved in plasma (C_p). The amount of capillary oxygen (C_c) depends on the delivery of oxygen from upstream arteries (C_a) and the amount transported to tissue (last term in Eq. (1)). The transport of oxygen to tissue (last term in Eq. (1)) was assumed to depend on the concentration difference between plasma and tissue oxygen concentration (C_t) as well as the capillary oxygen permeability (P) and surface area of exchange (S_c). In Eq. (1), the gradient of oxygen along the direction of the vessel was assumed to be approximately linear, such that the capillary concentration of oxygen (C_c) was represented by its average concentration. The Hill equation was used to relate the dissolved oxygen in plasma to that bound to hemoglobin and the kinetics of this association and dissociation were considered to be instantaneous (Popel 1989). The average concentration of tissue oxygen (C_t) depends on the amount of oxygen transported from the vessel and the consumption in tissue (CMR_{O2}). The relative volumes of these compart-

Table 1
Oxygen exchange model parameters

Parameter	Description	Typical value	Reference
C_c	Average capillary oxygen concentration	Calculated	
V_c	Capillary volume	1 ml/100 g	Valabregue et al., 2003
F	Cerebral blood flow	150 ml/min/100 g [a]	Kim et al., 2007
C_a	Arterial oxygen concentration	7.3 mM (87 mmHg [b])	
PS_c	Capillary permeability, surface area product	7000 ml/min/100 g	Liu et al., 1994; Kassissia et al., 1995
C_p	Average capillary plasma oxygen concentration	Calculated	
C_t	Average tissue oxygen concentration	0.046 mM (32.8 mmHg [a])	Average measured value
V_t	Tissue volume	97 ml/100 g	Valabregue et al., 2003
CMR_{O2}	Cerebral metabolic rate of oxygen consumption	6.4 ml/min/100 g [a]	Calculated value
[Hb]	Hemoglobin concentration	1.99 mM [a]	Average measured value
α	Oxygen solubility constant	1.39×10^{-3} mM/mmHg	Valabregue et al., 2003
P_{50}	Oxygen tension at half hemoblogin saturation	38 mmHg	Gray and Steadman, 1964
H	Hill exponent	2.73	Valabregue et al., 2003

[a] Baseline value.
[b] Equivalent tension.

ments contribute to the dynamics of capillary and tissue oxygenation.

$$V_c\frac{dC_c(t)}{dt} = 2F(t)(C_a - C_c(t)) - PS_c\big(C_p(t) - C_t(t)\big) \quad (1)$$

$$V_t\frac{dC_t(t)}{dt} = PS_c\big(C_p(t) - C_t(t)\big) - \mathrm{CMR_{O2}}(t) \quad (2)$$

$$C_c = C_p(t) + \frac{4[\mathrm{Hb}]}{1+\left(\frac{\alpha P_{50}}{C_p}\right)^h} \quad (3)$$

The variable F represents the dynamic changes in blood flow, V_c and V_t represent the capillary and tissue volumes, respectively, and [Hb], α, P_{50} and h represent the hemoblogin concentration, oxygen solubility constant, tension of half hemoglobin saturation, and Hill exponent, respectively. The experimental data, which consisted of tissue P_{O2} and LDF measurements, corresponded to $C_t(t)$ and $F(t)/F_0$ in the model, respectively, where F_0 is the baseline blood flow. The P_{O2} measurements were converted to concentration using the oxygen solubility constant (i.e. $C_t=\alpha P_{O2}$, Henry's Law). The values of the unknown model parameters (i.e. V_c, F_0, C_a, PS_c, V_t, CMR_{O20}, α, P_{50}, h) were determined considering the model and its spatial extent (see below), and previously reported values in the literature (see Table 1).

The spatial extent of the model depends on the spatial sensitivity of the measurements, namely LDF and P_{O2}. Both of these methodologies have spatial sensitivities on the order of hundreds of microns. Since the P_{O2} probe was placed about 300 μm from the cortical surface and capillary lengths are about 250 μm (Vovenko 1999), the input arterial oxygenation (C_a) corresponds to that of small arterioles. Vovenko reported the mean oxygen tension to be 81, 68, 41 and 41 mmHg in large pial arteries (90 μm diameter), surface arterioles (26 μm diameter), surface venules (62 μm diameter) and large pial veins (516 μm diameter), respectively, in the rat brain (Vovenko 1999; see Table 2). The average systemic arterial blood oxygenation was measured to be 86 mmHg in that study. Therefore, the input arterial oxygenation for the model in this study was determined using the average measured systemic arterial oxygen tension multiplied by the ratio between the penetrating arteriole oxygen tension and the systemic arterial oxygen tension reported by Vovenko (i.e. 68/86=0.79). Similarly, the output venous oxygenation for the tissue P_{O2} sensitivity area corresponds to that of small venules, such as emerging venules and small cortical veins. The oxygen tension in this size veins was measured by Vovenko to be 41 mmHg. Another important unknown parameter is the baseline blood flow level (F_0). The CBF baseline has been measured in our laboratory to be 150 ml/min/100 g using MRI in a different group of animals but under similar control experimental conditions (Kim et al., 2007). Therefore, this value was also assumed to hold for the average data under control conditions in this work. When using suppressed CBF

Table 2
Measured P_{O2} values in cerebral blood vessels reported by Vovenko, 1999 and tissue P_{O2} from this study

Location	Measured P_{O2} value in this study (S_{O2}) (% relative to systemic arterial P_{O2})	Reported P_{O2} value by Vovenko, et al. (S_{O2}) (% relative to systemic arterial P_{O2})
Systemic Arterial	110 (94.9%) (100%)	86 (N/A) (100%)
1° Branching artery (D=45 μm)		81 (94%) (94%)
2° Branching artery (D=33°μm)		79 (94%) (92%)
3° Branching artery (D=26 μm)		76 (93%) (88%)
4° Branching artery (D=13 μm)		68 (89%) (79%)
5° Branching artery (D=7 μm)		61 (84%) (71%)
Mean capillaries		50 (63%) (58%)
Tissue	32 (N/A) (29%)	
5° Branching vein (D=13 μm)		38 (54%) (44%)
4° Branching vein (D=31 μm)		41 (59%) (48%)
3° Branching vein (D=71 μm)		40 (57%) (47%)
2° Branching vein (D=145 μm		39 (57%) (45%)
1° Branching vein (D=258 μm)		41 (59%) (48%)

condition data, this baseline blood flow level was adjusted by the relative change in LDF signal between control and suppressed CBF conditions. Lastly, the permeability-surface area (PS_c) parameter value was obtained from the literature and assumed to represent the control condition permeability-surface area (Kassissia et al., 1995). Under suppressed CBF conditions, the permeability-surface area product was increased to 7900 ml/min/100 g (from 7000 ml/min/100 g) to match the baseline metabolic rate of the control condition. The baseline CMR_{O2} (CMR_{O20}) value was then calculated using the model. See Table 1 for all other parameter values.

Data analysis

After recording the LDF and tissue P_{O2} data, the various trials within each experimental condition were averaged across animals and the resulting time series were low-pass filtered with a 5 Hz rectangular cutoff. The tissue P_{O2} data were corrected for the measurement lag (measured independently to be 1.0 s to 90% of the final amplitude for the oxygen sensor used) by deconvolution with an exponential function prior to filtering. Small linear trends were removed from the average data considering 5 s periods temporally located 5 s prior to stimulation and 65 s after stimulation onset. The resulting average tissue P_{O2} and LDF data were used for the two steps of the analysis performed and depicted in Fig. 1. The first step (I) consisted of determining the changes in the tissue oxygen consumption with evoked stimulation. The second step (II) consisted of estimating the changes in tissue oxygen delivery with evoked stimulation. These two steps were repeated for several cases investigated below. All computations were implemented and performed using Matlab (Mathworks Inc., Natick MA).

Step I: CMR_{O2} calculation

The average tissue P_{O2} and LDF data obtained under suppressed CBF conditions were used to represent the tissue demand of oxygen and determine $CMR_{O2}(t)$ using the oxygen exchange model (Eqs. (1), (2) and (3); Step I in Fig. 1). The baseline blood flow (F_0) was modified by the corresponding increase in baseline blood flow measured by LDF between control and suppressed CBF conditions in each animal tested. The baseline arterial oxygen tension was calculated using the 79% ratio relative to the average systemic arterial oxygen tension for this condition (116 mmHg *0.79=92 mmHg). Lastly, the permeability-surface area product was increased to 7900 ml/min/100 g to match the control condition CMR_{O2} baseline level. The remaining model parameters were not changed (see Table 1), with the exception of specific model parameters tested in Step II.

Step II: Tissue O_2 delivery estimation and comparison

The dynamics of tissue oxygen delivery were investigated as follows. The model prediction of the tissue P_{O2} under control conditions was calculated using Eqs. (1), (2) and (3), the parameters in Table 1, the measured LDF data under control conditions, and the

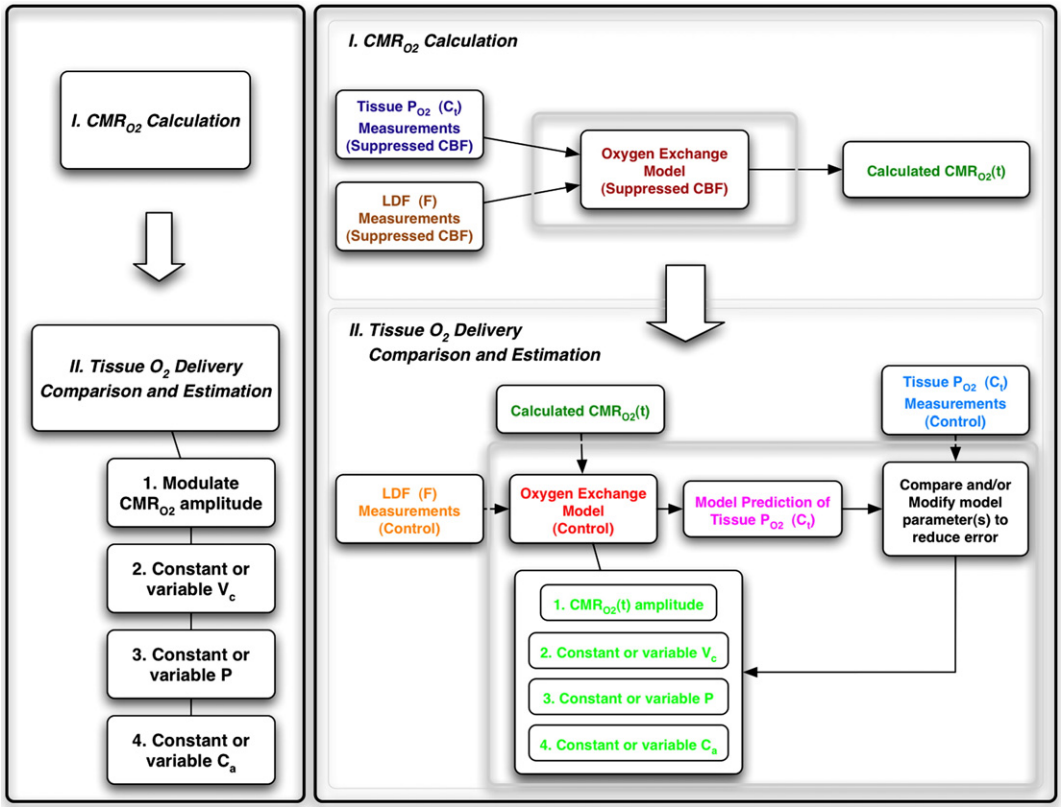

Fig. 1. Schematic of the data analysis performed. The box on the left depicts the flow summary of the major steps. The box on the right parallels the flow summary on the left with a more detailed flow of the data given to the model in order to determine the oxygen consumption in Step I and the data given to the model to estimate the corresponding tissue oxygen delivery in Step II for each parameter investigated.

CMR_{O2} calculated in Step I (see Fig. 1). Then, the model prediction of the tissue P_{O2} was compared to the measured tissue P_{O2} data under control conditions ($(C_t)_{control}$) by the mean squared error (MSE). To examine and minimize the difference between the predicted and measured tissue oxygen tension, various model parameters were modified; specifically, four possibilities (also referred to as cases throughout the manuscript) were considered:

CMR_{O2} change. The first possibility evaluated the amplitude of the CMR_{O2} response under control conditions (represented by the parameter κ in Eq. (4)). In this case, the amplitude of the relative CMR_{O2} change was manipulated using a non-linear least-squares algorithm that minimized the difference between the predicted tissue P_{O2} and measured tissue P_{O2} data under control conditions (see Eq. (4)).

$$(\mathrm{CMR_{O2}}(t,\kappa))_{\mathrm{prediction}} = \underset{\kappa}{\mathrm{argmin}} \left\{ \left((C_t(t))_{\mathrm{control}} - C_t(\kappa, \mathrm{CMR_{O2}}(t), F(t), \ldots) \right)^2 \right\} \quad (4)$$

Capillary volume and surface area. The second possibility evaluated whether changes in the capillary surface area can account for the discrepancies by manipulating the capillary volume (V_c) and surface area (S_c) parameters. In this case the vessel was assumed to be cylindrical in shape and three fixed capillary volumes were tested: 0.5, 1.0 and 5.0 ml/100 g. The appropriate $CMR_{O2}(t)$ was first calculated (Step I) for each V_c value tested. A dynamic capillary volume (and surface area) was also tested assuming a 1.0 ml/100 g resting capillary volume ($V_c = V_c(t)$). In this case, a non-linear optimization algorithm was used to minimize the difference between the predicted tissue oxygenation and the measured tissue oxygenation under control conditions by freely manipulating the capillary volume and surface area parameters as a function of time (see Eq. (5)).

$$V_c(t) = \underset{V_c}{\mathrm{argmin}} \left\{ \left((C_t(t))_{\mathrm{control}} - C_t(V_c(t), S_c(V_c)\mathrm{CMR_{O2}}(t), F(t), \ldots) \right)^2 \right\} \quad (5)$$

Capillary permeability. The third possibility evaluated whether the permeability (P) can account for the discrepancies by manipulating this parameter. Fixed permeability values that correspond to permeability-surface area products of 3500, 7000 and 14,000 ml/min were tested in this case. The appropriate $CMR_{O2}(t)$ was first calculated (Step I) for each permeability value tested. Additionally, a dynamic permeability ($P = P(t)$) was also investigated as in Case 2, assuming a baseline permeability-surface area product of 7000 ml/min (see Eq. (6)).

$$P(t) = \underset{C_a}{\mathrm{argmin}} \left\{ \left((C_t(t))_{\mathrm{control}} - C_t(P(t), \mathrm{CMR_{O2}}(t), F(t), \ldots) \right)^2 \right\} \quad (6)$$

Arterial oxygenation. The fourth possibility evaluated whether changes in the arterial oxygen tension entering the compartment (captured in the term C_a) could account for the discrepancies. In this case, several fixed arterial oxygen tensions were tested: the average systemic arterial oxygen tension, 87, 70 and 60 mmHg. The appropriate $CMR_{O2}(t)$ was first calculated (Step I) for each arterial oxygen tension value tested. A dynamic arterial oxygen concentration ($C_a = C_a(t)$) was also tested as in Case 2 for a resting input arterial blood oxygen tension of 87 mmHg (see Eq. (7)).

$$C_a(t) = \underset{C_a}{\mathrm{argmin}} \left\{ \left((C_t(t))_{\mathrm{control}} - C_t(C_a(t), \mathrm{CMR_{O2}}(t), F(t), \ldots) \right)^2 \right\} \quad (7)$$

In those cases where a variable function of time was estimated ($V_c(t)$, $P(t)$, $C_a(t)$), free parameters were temporally set every 0.5 s spanning a total of 58 s, starting 3 s prior to stimulation onset. A total of 116 parameters were estimated in these cases. For minimization, the estimated time course was linearly interpolated to the measured data to compute the error.

The different cases were compared using two criteria: (1) the MSE between the measured and the model fit of the tissue P_{O2} under control conditions, and (2) the magnitude and temporal shape of the estimated model parameters compared to their known physiological values. After selecting the case that is most representative of the physiological changes using the above criteria, the tissue tension time course of oxygen delivery was computed using the model parameters of that specific case while fixing the CMR_{O2} time series to its baseline value ($CMR_{O2}(t) = CMR_{O20}$; see Eq. (8), Table 1). The temporal properties of the computed tissue oxygen delivery were then compared to the measured change in blood flow under control conditions and to the measured change in tissue oxygen tension measured under suppressed CBF conditions, indicative of oxygen consumption. The dynamics of blood oxygen delivery and tissue consumption with evoked stimulation can be expressed in terms of the model's average tissue oxygen concentration (C_t in Eqs. (1) and (2)). Since the suppressed CBF condition essentially maintains CBF constant with evoked stimulation, the experimental conditions can also be incorporated into these expressions as follows:

Tissue O_2 due to oxygen delivery:

$$(C_t(t; \mathrm{CMR_{O2}}(t) = \mathrm{CMR_{O2}}))_{\text{control condition}} \quad (8)$$

Tissue O_2 due to oxygen consumption :

$$(C_t(t))_{\text{suppressed CBF condition}} \quad (9)$$

Results

The average LDF and tissue P_{O2} time series under control and suppressed CBF conditions are presented in Fig. 2. The average blood flow signal recorded using LDF increased by 48.8% due to somato-sensory stimulation under control conditions (left panels A and B). Temporally, the response peaked 6.8 s after stimulation onset, started decreasing with stimulation offset and returned to baseline 20 s after stimulation offset. The blood flow change was mostly suppressed under suppressed CBF conditions, increasing by only 2.1% with somato-sensory stimulation. The tissue P_{O2} increased from a baseline of 32.8 mmHg to 41.9 mmHg (+27.7%, Δ=9.1 mmHg) due to somato-sensory stimulation under control conditions (right panels C and D). Temporally, the response started increasing 2 s after stimulation onset and peaked 9.8 s after stimulation onset. The initial undershoot typical of many evoked tissue P_{O2} responses was not significant. A post-stimulus undershoot was observed and reached a minimum of 32.0 mmHg (−2.4%), 30 s after stimulus offset, and returned to baseline 54 s after stimulation offset. Under suppressed CBF conditions, the tissue P_{O2} signal decreased from its baseline level of 42.5 mmHg to 37.7 mmHg

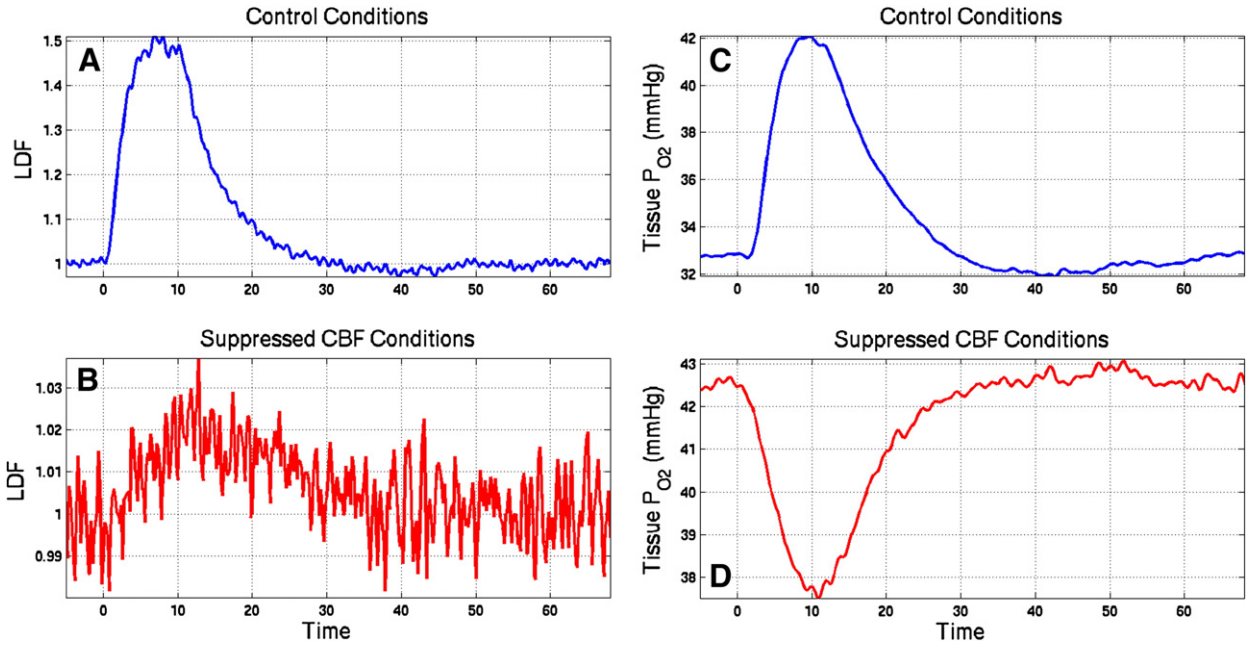

Fig. 2. Average measured LDF (relative change; left panels A and B) and tissue P_{O2} data (in mm Hg; right panels C and D) under control (top panels A and C) and suppressed CBF conditions (bottom panels B and D). Evoked stimulation under control conditions produced an average increase of 48.8% and 27.7% in LDF and tissue P_{O2} signals, respectively. The blood flow change was mostly suppressed with the administration of sodium nitroprusside (sNP; bottom-left panel B) while a decrease in tissue P_{O2} of −11.7% was measured due to the oxygen consumption response produced by evoked stimulation (bottom-right panel D).

(−11.3%, Δ=4.8 mmHg) following stimulation onset. Temporally, no significant lag was observed in the response, it reached the minimum 10.8 s after stimulation onset (0.8 s after stimulation offset) and returned to baseline 22 s after stimulation offset.

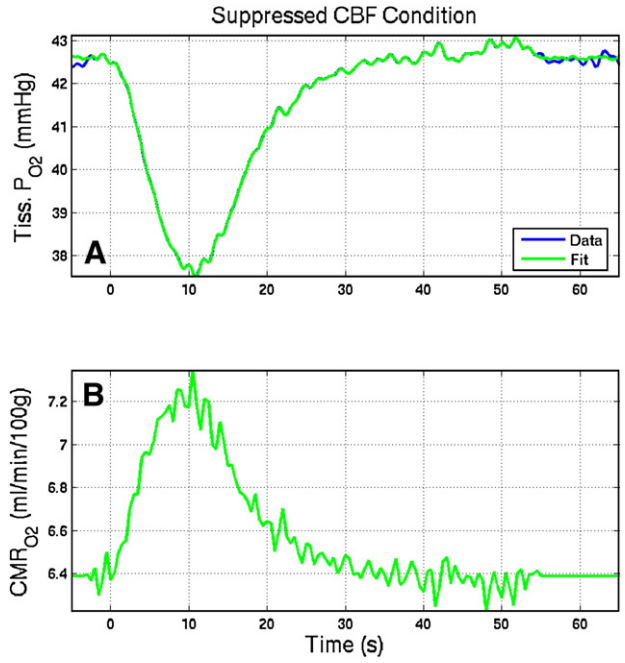

Fig. 3. Calculated tissue CMR_{O2} response (in ml/min/100 g; panel B) using the model and the LDF and tissue P_{O2} (mmHg) data under suppressed CBF conditions. The calculated CMR_{O2} response was truncated to its baseline value 55 s after stimulus onset and over 3 s prior to stimulus onset.

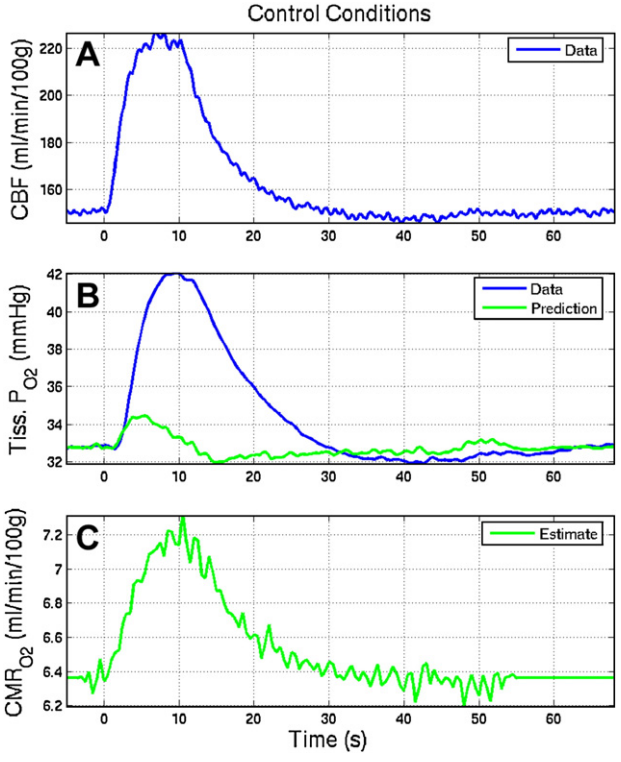

Fig. 4. Prediction of the control condition tissue P_{O2} (middle panel B) using the oxygen exchange model and the LDF data under control conditions ($F=F_0$*LDF; top panel A) and the calculated CMR_{O2} response under suppressed CBF conditions (bottom panel C) as inputs. It is evident that the model prediction of the tissue P_{O2} (middle panel B) does not represent the data.

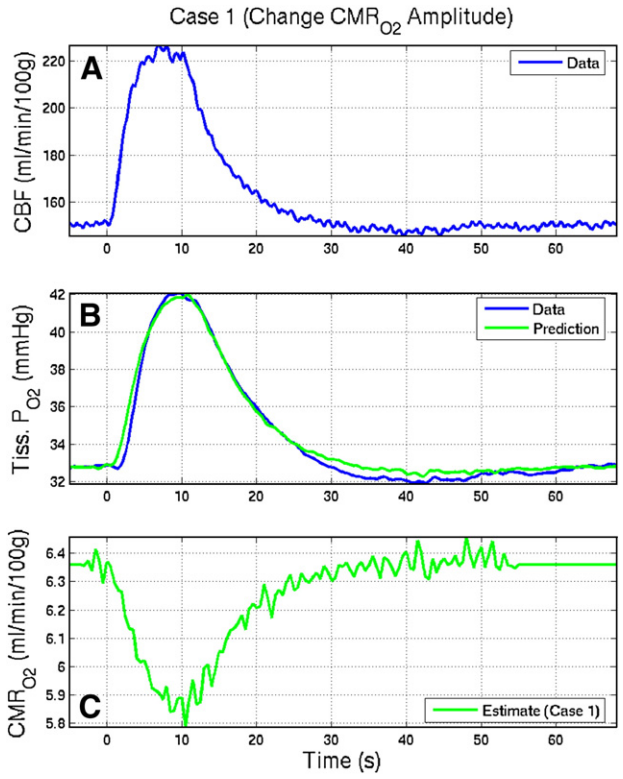

Fig. 5. Estimate of the required CMR_{O2} response amplitude change that best represents the measured tissue P_{O2} response under control conditions (Case 1; panel B). Assuming that only the amplitude of the CMR_{O2} response is incorrect, a −7.8% change in the CMR_{O2} response under control conditions would be necessary to represent the tissue P_{O2} data.

The tissue oxygen consumption time course (see Eq. (2) of the model) was then calculated using the average LDF and tissue P_{O2} data under suppressed CBF conditions. The parameters in Table 1 were adjusted to represent the suppressed CBF condition. Specifically, the baseline blood flow was increased to 203.3 ml/min/100 g to represent the 35.6% increase in LDF baseline between suppressed CBF and control conditions. The input arterial oxygen tension was set to 92 mmHg and the CMR_{O2} baseline was calculated to be 6.4 ml/min/100 g considering a permeability, surface area product of 7900 ml/min/100 g. The calculated $CMR_{O2}(t)$ is presented in Fig. 3 (bottom panel B). Temporally, the $CMR_{O2}(t)$ time course is similar to the tissue P_{O2} time course, leading the tissue P_{O2} response by 0.8 s at half-maximum. It peaked around 7.2 ml/min/100 g (+12.9%) at the end of the stimulation period (10 s after onset) and returned to baseline 25 s after stimulation offset.

The dynamics of the tissue oxygen delivery were investigated using the model in Eqs. (1), (2) and (3), along with the average LDF and tissue P_{O2} data under control conditions and the CMR_{O2} time course calculated above. Initially, the model was tested using the parameters in Table 1. The discrepancy between the measured and predicted tissue P_{O2} under control conditions is presented in Fig. 4. It is evident that the tissue oxygen delivery predicted by the model is not sufficient to explain the experimental data. An exhaustive investigation was then performed from which four possibilities were investigated. The first possibility was to change the amplitude of the CMR_{O2} response relative to baseline that best fit the data (Fig. 5). Surprisingly, the CMR_{O2} change was estimated to be −7.8% under control conditions. A negative change in the CMR_{O2} response is very unlikely since most reports have found at least positive responses (Davis et al., 1998; Fox et al., 1988; Kim et al., 1999; Shulman et al., 2001), similar to the CMR_{O2} calculated above under suppressed CBF conditions.

The second possibility investigated whether the capillary volume and surface area could explain the observed discrepancy. Three fixed capillary volume and corresponding surface area values were individually tested: 0.5, 1.0 and 5.0 ml/100 g (see Fig. 6, panel A). A capillary volume of 5 ml/100 g (with its corresponding surface area increase) is closer to the measured tissue oxygen tension; however, an even higher capillary surface area and volume would be necessary. A dynamic capillary volume (and surface area) was also tested (Fig. 6, panels B–D) and an

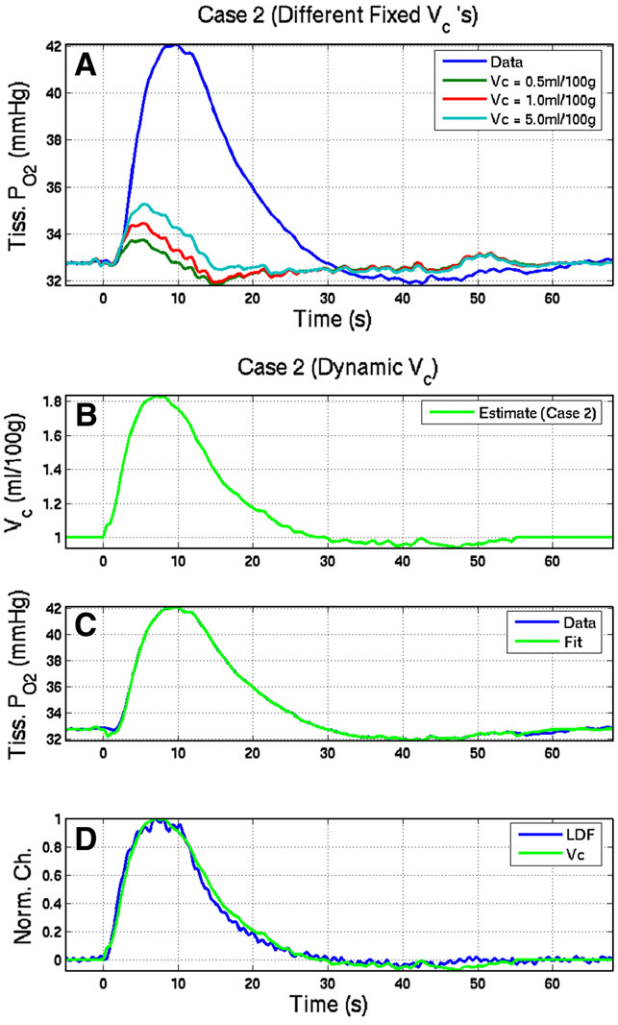

Fig. 6. Effect of the capillary volume and surface area on the delivery of oxygen to tissue (Case 2). Different fixed levels of capillary volume and their corresponding surface area were tested (panel A). Although a larger capillary volume delivers more oxygen tissue, it is not sufficient to represent the tissue P_{O2} data under control conditions (light blue line, panel A). A dynamic capillary volume (and its corresponding surface area) was also tested (panels B–D). A 82.0% increase in capillary volume (baseline level of 1 ml/100 g; panel B) is able to represent the measured tissue P_{O2} data (panel C).

82.0% change in the capillary volume (34.9% in surface area) to 1.820 ml/100 g was estimated to fit the tissue P_{O2} data under control conditions with very low residual error. Temporally the change in capillary volume matched very well with the changes in blood flow indicated by the LDF data (panel D). This increase in capillary volume is higher than most reports in the literature (Wu et al., 2003; Peppiatt et al., 2006).

The third possibility investigated whether the permeability could explain the observed discrepancy. Three constant permeabilities were individually tested: 3500, 7000 and 14,000 ml/min/100 g (Fig. 7, panel A). As expected, the highest constant permeability tested (14,000 ml/min/100 g) supplies the largest amount of oxygen to tissue; however, a much larger constant permeability would be necessary to describe the tissue P_{O2} behavior represented in the data. A dynamic permeability was also tested (Fig. 7, panels B–D). Interestingly, the permeability was

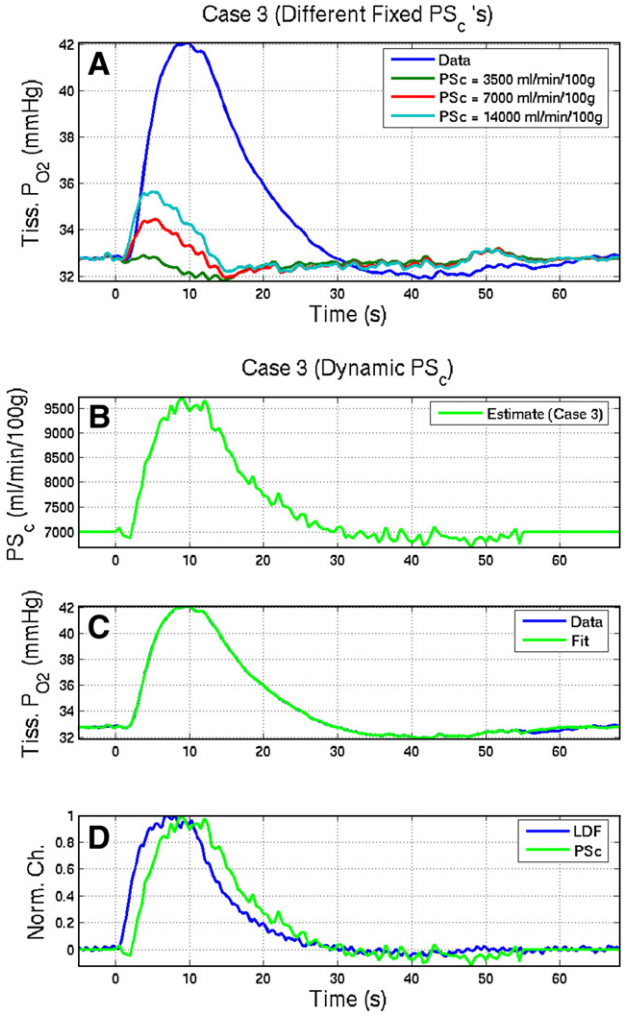

Fig. 7. Effect of the capillary permeability on the delivery of oxygen to tissue (Case 3). Several fixed permeability levels were tested and compared to the measured tissue P_{O2} data under control conditions. Although a larger permeability delivers more oxygen to tissue, it is not sufficient to represent the tissue P_{O2} data (panel A). A dynamic permeability was also tested and a 36.7% increase in permeability was found to represent the data (panels B–D).

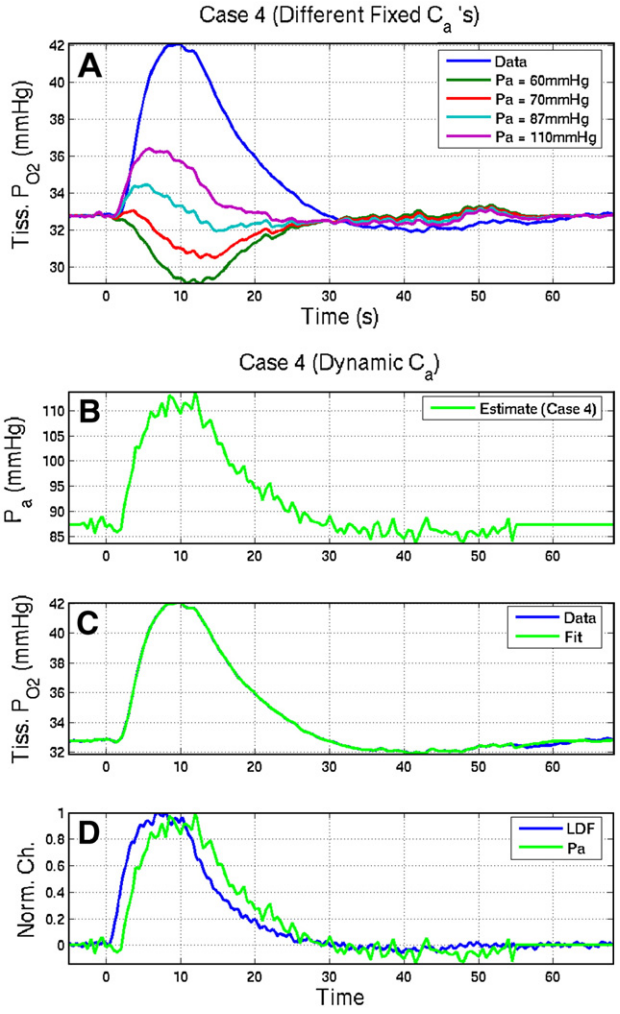

Fig. 8. Effect of the input arterial oxygenation on the oxygen delivery to tissue (Case 4). Several fixed input arterial oxygen tension levels were tested and compared to the measured tissue P_{O2} data. A higher input arterial oxygen tension delivers more oxygen to tissue but it was not sufficient to represent the data (panel A). A dynamic input arterial oxygenation was also tested and a 27.3% increase in the input arterial oxygen tension was found to represent the tissue P_{O2} data under control conditions (panels B–D).

required to increase by 36.7% to represent the data and this change was delayed by 1.7 s compared to the change in the blood flow signal (LDF) at half-maximum (panel D). However, if the change in permeability was produced by changes in blood velocity, we would expect the change in permeability and blood flow to roughly coincide.

The fourth possibility investigated whether a different input arterial oxygenation could describe the tissue P_{O2} changes observed in the data under control conditions. Four constant input arterial oxygen tension levels were tested: 110 (systemic), 87, 70 and 60 mmHg (Fig. 8, panel A). As expected, the highest input arterial oxygen tension tested supplied the highest amount of oxygen to tissue, but, again, a significantly larger input arterial oxygen tension would be necessary to describe the data. A dynamic arterial oxygen tension was also tested (Fig. 8, panels B–D). A +27.3% increase in the input arterial oxygen tension (up to 110.9 mmHg) was estimated to best represent the data. Interestingly, the estimated input arterial

oxygen tension was estimated to reach the systemic arterial oxygen tension and was also delayed with respect to the measured blood flow signal (LDF) by 1.4 s at half-maximum. The change in arterial oxygenation represented in this case takes place in upstream arterioles and may be susceptible to delays by the arterial transit time to the capillary bed.

Finally, the tissue oxygen delivery was calculated by fixing the CMR_{O2} response to its baseline level (i.e. no CMR_{O2} change) and the dynamic arterial oxygenation obtained in Case 4 (Fig. 9). Equivalent results were obtained when using the dynamic capillary volume changes estimated for Case 2 (results not shown). These two cases have physiological significance and very low MSE. The computed tissue oxygen delivery required an increase to 47.8 mmHg (from 32.8 mmHg or +45.7%) to meet the estimated tissue demand under control conditions. This can be compared to the estimated drop in tissue P_{O2} to 27.2 mmHg (from 32.8 mmHg or −17.1%; recall that the calculated CMR_{O2} has been assumed to be the same between suppressed CBF and control conditions). The ratio between the change in oxygen tension due to delivery by CBF and oxygen consumption due to CMR_{O2} was calculated to be 2.7 (|+45.7%/−17.1%|). Temporally, the computed change in tissue oxygen delivery under control conditions followed the measured tissue P_{O2} change under suppressed CBF conditions, leading the latter by only 0.2 s at half-maximum (Fig. 9). However, the computed change in tissue oxygen delivery lagged the blood flow response measured using LDF by 2.2 s at half-maximum. This temporal difference is dominated by the difference in volume fractions between vessel and tissue. More importantly, the combination of the computed tissue P_{O2} from delivery and tissue P_{O2} from consumption does not show any transient deficiency in tissue oxygenation.

Discussion

The dynamics of the blood oxygen delivery and tissue oxygen consumption produced by the evoked stimulation of the rat somatosensory cortex were investigated using tissue P_{O2} and LDF measurements, and an oxygen exchange model. The temporal changes in tissue P_{O2} computed for oxygen delivery were very similar to those of the measured tissue P_{O2} response under control conditions and suppressed CBF conditions. More importantly, the results showed the blood oxygen delivery predicted by the model exceeds the delivery of oxygen calculated using commonly adopted assumptions (see Figs. 4 and 9). The amplitude of the estimated tissue P_{O2} of oxygen delivery was about 2.7x larger than that estimated for oxygen consumption under control conditions. Interestingly, the large increase in tissue oxygen tension was found to probably require the recruitment of upstream oxygen from larger arterioles and arteries as well as increases in the vascular volume at the oxygen exchange sites (e.g. capillaries). In addition, the time courses of both the measured tissue P_{O2} (under control conditions) and the difference between the estimated tissue P_{O2} due to oxygen delivery and consumption (see Fig. 9) did not show any transient oxygen deficits that would require the large changes in oxygen delivery estimated in this work.

The investigation of the dynamics of oxygen delivery produced by evoked stimulation is not trivial. There are at least two general methods that could be devised to study blood oxygen delivery: an

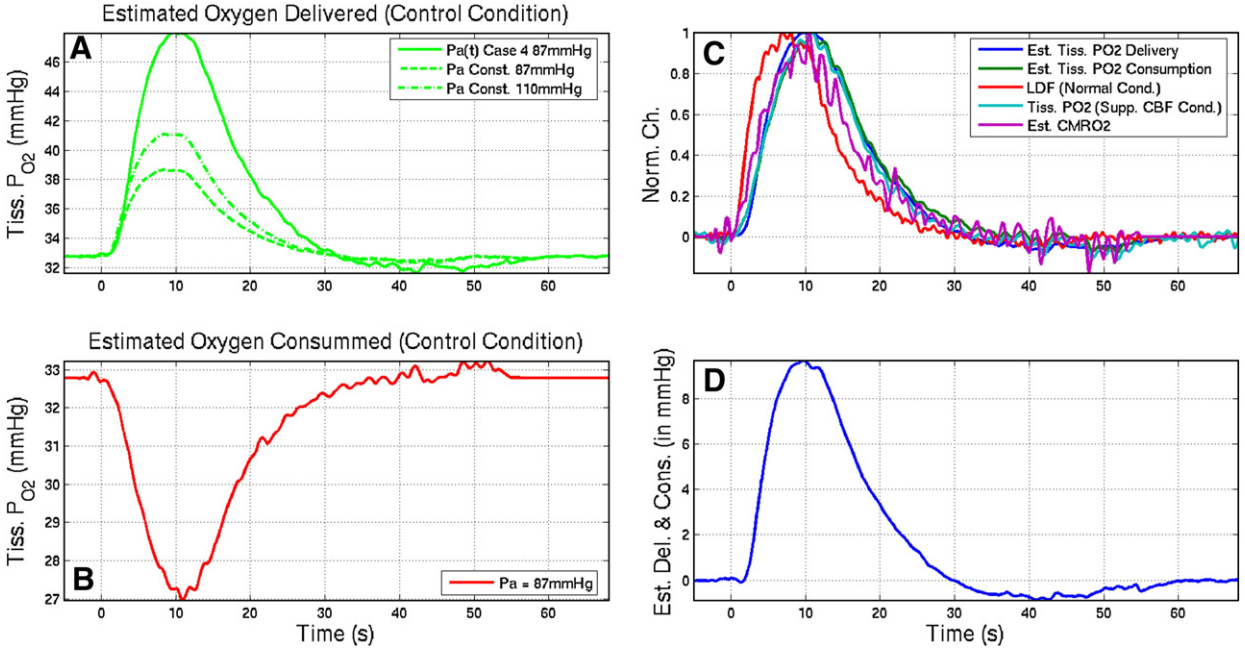

Fig. 9. Estimated tissue oxygen delivery and consumption under control conditions (top-right panel A, solid green line, and bottom-right panel B, red solid line, respectively). These were calculated using the suppressed CBF condition data and the results from Case 4 (although the latter are not dependent on the specific case used since all cases substantially lowered the mean squared error). The temporal changes between the estimated tissue P_{O2} due to delivery (no change in CMR_{O2}), tissue P_{O2} due to consumption (no change in CBF), LDF data under control conditions, tissue P_{O2} data under suppressed CBF conditions and estimated CMR_{O2} were compared relative to their normalized changes (top-right panel C). As expected, the combination of tissue P_{O2} due to delivery and tissue P_{O2} due to consumption shows no transient deficits in tissue oxygenation (bottom-right panel D).

experimental design that manipulates blood flow in similar fashion to evoked stimulation experiments in the absence of oxygen consumption changes, or a normal experimental design that incorporates a known consumption of tissue oxygen. In this work, the latter was adopted using the tissue P_{O2} measurements under suppressed CBF conditions to determine the tissue oxygen consumption. An oxygen exchange model was then used to calculate the dynamics of oxygen delivery under control conditions.

Consequently, the results presented in this work relied on two general assumptions. The first assumption was that the CMR_{O2} calculated under suppressed CBF conditions is the same as that under control conditions. This condition, as used in our experiments, has been shown to not affect the tissue electrical activity (i.e. field potentials and spiking activity) (Fukuda et al., 2006; Masamoto et al., 2007). The second assumption was that the model accurately represents the physiology as measured by LDF and the P_{O2} sensor. An inherent limitation of the combination of these methodologies is the sampling of potentially different volumes. This difference was minimized by positioning the probes as close as possible. In addition, the P_{O2} sensor placement criteria also included avoiding large visible vessels. Since the vascular volume is a small fraction of the tissue volume and small vessels tend to be spatially distributed with random orientations (particularly capillaries), the average P_{O2} sensor data most likely represents the average tissue oxygen tension. Lastly, the spatial extent of the area of activity determined by optical imaging exceeded the spatial extent of these techniques. Therefore, similar tissue areas were considered to be sampled by both LDF and P_{O2} measurements.

A drawback of the model is the number of parameters that were not measured. Nonetheless, values for these parameters have been reported in the literature and most of the parameters have physiological constraints for their values. Of critical importance are the baseline blood flow (F_0), surface area (S_c) and input arterial oxygenation (C_a). The baseline blood flow in the somato-sensory cortex was measured by our group to be 150 ml/min/100 g under similar experimental conditions (Kim et al., 2007). The surface area and the permeability values were adopted from the literature (Liu et al., 1994; Kassissia et al., 1995). There are several reports for these values in the literature and the values selected are close to their respective average values. The model's input arterial oxygen tension is not known but it is bounded by the systemic arterial oxygen tension (110 mmHg in this work) and the tissue oxygen tension (32 mmHg in this work). Moreover, it depends on the measurement volume of the oxygen sensor, and, therefore, should correspond to the oxygen tension of mid-size and small arterioles. A ratio of 79% relative to the mean systemic arterial oxygen tension was used as the criteria to approximate the arterial P_{O2} in this work. Additional arterial P_{O2} values were also tested to examine the sensitivity of the results to this parameter and no significant differences were found.

Four cases were considered as possible inaccuracies or misrepresentations of the oxygen exchange model. The first case determined the required amplitude of the change in the CMR_{O2} response that would describe the data. A negative change was found to be necessary, but most reports in the literature point to either positive or no changes in the CMR_{O2} response (Davis et al., 1998; Fox et al., 1988; Hoge et al., 1999; Kim et al., 1999; Shulman et al., 2001). The second case determined which constant or variable changes in the capillary volume and surface area is able to describe the data. The results showed that a capillary volume change of about 82% concomitant with the changes in blood flow is able to describe the control condition tissue P_{O2} data. Although it was thought that the capillary volume does not change, there is increasing evidence of changes in the capillary volume with changes in blood flow (Wu et al., 2003; Peppiatt et al., 2006), though none with changes as large as those found for this case. The third case determined which constant or variable oxygen permeability is able to describe the data. The results showed that an increase in the capillary permeability of about 37% is able to describe the data; however, it is unlikely that the permeability would increase (or lag) with increases in blood flow within the compartment. In fact, decreases in the permeability might be more likely. The fourth case determined which constant or variable input arterial oxygenation is able to describe the data. The results showed that a dynamic input arterial oxygen tension that increases by 27% from 87 mmHg to 110 mmHg was able to describe the data. Temporally, this change also lagged the blood flow change; however, this change is being produced upstream and could be sensitive to changes in the upstream transit time. After evaluating the results from each of the cases tested, the changes in capillary volume and input arterial oxygenation are the most likely to influence the delivery of oxygen to tissue.

Following these findings, the changes in the input arterial oxygenation within the tissue P_{O2} compartment were investigated by implementing an additional model compartment of the upstream arterial vasculature. This exercise aimed to determine whether the changes in the arterial oxygen tension can accommodate the changes determined in Case 4. It was assumed that this upstream compartment experiences the same change in blood flow and that enough oxygen escapes the vascular compartment such that the upstream end-arterial oxygen tension is the input oxygen tension of the original model (i.e. 87 mmHg with a PS of 620 ml/min/100 g). Further, the changes in blood flow were assumed to be carried out solely by changes in blood velocity and that there were no changes in oxygen consumption in this compartment such that the changes in blood flow maximally increase the end-arterial oxygenation level. The end-arterial oxygenation was predicted to increase by 6 mmHg to 93 mmHg due to the change in blood flow. If the desired upstream end-arterial oxygenation is 70 mmHg instead of 87 mmHg, the end-arterial oxygenation is predicted to increase by 8 mmHg to 78 mmHg (PS of 1910 ml/min/100 g). Regardless, the changes in the modeled upstream arterial oxygen tension are not sufficient to account for the required changes in tissue P_{O2}. This suggests that increases in the capillary volume contribute at least a significant portion of the increased oxygen delivery to tissue. Given the magnitude of the required change in capillary volume, a combination of both possibilities (Cases 2 and 4) would probably be more physiologically feasible. A preliminary model was then tested combining the upstream vascular compartment tested above with a variable capillary volume (Case 4). Considering a 6 to 8 mmHg increase in arterial oxygen tension due to increases in blood flow (with input oxygen tensions of 87 and 70 mmHg, respectively, into the capillary compartment) would require increases in the capillary volume of around 55 and 45%, respectively, to completely describe the tissue P_{O2} data.

The changes in oxygen consumption described by the model in Eqs. (1), (2) and (3) were calculated using the tissue P_{O2} and LDF data under suppressed CBF conditions. In this condition, the changes in blood flow (LDF) were mostly suppressed and a decrease in tissue P_{O2} produced by the CMR_{O2} response was observed. Temporally, the changes in CMR_{O2} were not rapid, relative to the stimulus; instead, they were comparable to the tissue P_{O2} changes under suppressed CBF conditions, leading the tissue P_{O2} response by 0.8 s at half-maximum. Similar findings using dynamic models were also reported

by Huppert et al., and Zheng, et al. (Huppert et al., 2007; Zheng et al., 2002). It is important to note that the model relied on the assumption of a linear longitudinal oxygen gradient along the vessel. This assumption implies that the changes in capillary oxygen concentration take place over an approximately linear range of the oxygen saturation curve. In addition, this assumption is known to over-estimate the absolute CMR_{O2} level.

The large increase in CBF with evoked brain activation has been hypothesized to take place because of the low mitochondrial P_{O2} and the diffusion limitation of oxygen transport (Buxton et al., 1997). Although the tissue P_{O2} was measured to be 32 mmHg in this work, this measurement represents the average P_{O2} over the sampling volume. A relatively small portion of this volume is occupied by mitochondria and, therefore, it is still possible that the large delivery of oxygen by CBF takes place to ensure that there is no oxygen deficit in mitochondria. This possible mechanism, however, is not evident in tissue P_{O2} measurements as performed in this work or in blood oxygenation measurements. Analyses regarding the oxygen consumption response are currently under investigation.

Conclusion

The dynamics of blood oxygen delivery and tissue consumption produced by evoked stimulation of the rat somato-sensory cortex were investigated. Tissue P_{O2} and LDF measurements were recorded under control and suppressed CBF conditions. These data were then analyzed using a model that described the transport of oxygen from blood to tissue and several hypothetical scenarios were considered. The amplitude of the estimated tissue tension of oxygen delivered was about 2.7x larger than the oxygen consumption under control conditions. The large increase in tissue oxygen tension was found to be larger than expected using typical model assumptions, suggesting that hemodynamic response also causes the recruitment of upstream oxygen from larger arterioles and arteries as well as increases in the vascular volume at the oxygen exchange sites. These findings need to be considered in the quantification of CMR_{O2} from blood oxygenation level changes at high spatial resolution (i.e. hundreds of microns).

Acknowledgments

This work was supported by NIH grants F32-NS056682 and R01-EB003375. The authors would also like to thank Dr. Mitsuhiro Fukuda and Dr. Luis Hernandez for their valuable comments and Dr. Ping Wang for his assistance with the experimental data collection.

References

Ances, B.M., Wilson, D.F., Greenberg, J.H., Detre, J.A., 2001. Dynamic changes in cerebral blood flow, O2 tension, and calculated cerebral metabolic rate of O_2 during functional activation using oxygen phosphorescence quenching. J. Cereb. Blood Flow Metab,. 21 (5), 511–516.

Arbit, E., DiResta, G.R., 1996. Application of laser Doppler flowmetry in neurosurgery. Neurosurg. Clin. N. Am. 7 (4), 741–748.

Buxton, R.B., Frank, L.R., 1997. A model for the coupling between cerebral blood flow and oxygen metabolism during neural stimulation. J. Cereb. Blood Flow Metab. 17 (1), 64–72.

Davis, T.L., Kwong, K.K., Weisskoff, R.M., Rosen, B.R., 1998. Calibrated functional MRI: mapping the dynamics of oxidative metabolism. Proc. Natl. Acad. Sci. U. S. A. 95 (4), 1834–1839.

Fatt, I., 1976. The polarographic oxygen sensor: Its theory of operation and its application in biology, medicine, and technology. CRC Press.

Fox, P.T., Raichle, M.E., Mintun, M.A., Dence, C., 1988. Nonoxidative glucose consumption during focal physiologic neural activity. Science 241 (4864), 462–464.

Fukuda, M., Wang, P., Moon, C.H., Tanifuji, M., Kim, S.G., 2006. Spatial specificity of the enhanced dip inherently induced by prolonged oxygen consumption in cat visual cortex: implication for columnar resolution functional MRI. Neuroimage 30 (1), 70–87.

Gray, L.H., Steadman, J.M., 1964. Determination of the oxyhaemoglobin dissociation curves for mouse and rat blood. J. Physiol. 175, 161–171.

Hoge, R.D., Atkinson, J., Gill, B., Crelier, G.R., Marrett, S., Pike, G.B., 1999. Linear coupling between cerebral blood flow and oxygen consumption in activated human cortex. Proc. Natl. Acad. Sci. U. S. A. 96 (16), 9403–9408.

Huppert, T.J., Allen, M.S., Benav, H., Jones, P.B., Boas, D.A., 2007. A multicompartment vascular model for inferring baseline and functional changes in cerebral oxygen metabolism and arterial dilation. J. Cereb. Blood Flow Metab. 27 (6), 1262–1279.

Kassissia, I.G., Goresky, C.A., Rose, C.P., Schwab, A.J., Simard, A., Huet, P.M., et al., 1995. Tracer oxygen distribution is barrier-limited in the cerebral microcirculation. Circ. Res. 77 (6), 1201–1211.

Kim, S.G., Rostrup, E., Larsson, H.B., Ogawa, S., Paulson, O.B., 1999. Determination of relative CMRO2 from CBF and BOLD changes: significant increase of oxygen consumption rate during visual stimulation. Magn. Reson. Med. 41 (6), 1152–1161.

Kim, T., Hendrich, K.S., Masamoto, K., Kim, S.G., 2007. Arterial versus total blood volume changes during neural activity-induced cerebral blood flow change: implication for BOLD fMRI. J. Cereb. Blood Flow Metab. 27 (6), 1235–1247.

Liu, C.Y., Eskin, S.G., Hellums, J.D., 1994. The oxygen permeability of cultured endothelial cell monolayers. Adv. Exp. Med. Biol. 345, 723–730.

Masamoto, K., Omura, T., Takizawa, N., Kobayashi, H., Katura, T., Maki, A., et al., 2003. Biphasic changes in tissue partial pressure of oxygen closely related to localized neural activity in guinea pig auditory cortex. J. Cereb. Blood Flow Metab. 23 (9), 1075–1084.

Masamoto, K., Kim, T., Fukuda, M., Wang, P., Kim, S.G., 2007. Relationship between neural, vascular, and BOLD signals in isoflurane-anesthetized rat somatosensory cortex. Cereb. Cortex. 17 (4), 942–950.

Masamoto, K., Vazquez, A., Wang, P., Kim, S.G., 2008. Trial-by-trial relationship between neural activity, oxygen consumption, and blood flow responses. Neuroimage 40 (2), 442–450.

Nagaoka, T., Zhao, F., Wang, P., Harel, N., Kennan, R.P., Ogawa, S., et al., 2006. Increases in oxygen consumption without cerebral blood volume change during visual stimulation under hypotension condition. J. Cereb. Blood. Flow. Metab. 26 (8), 1043–1051.

Peppiatt, C.M., Howarth, C., Mobbs, P., Attwell, D., 2006. Bidirectional control of CNS capillary diameter by pericytes. Nature 443 (12), 700–704.

Popel, A.S., 1989. Theory of oxygen transport to tissue. Crit. Rev. Biomed. Eng. 17 (3), 257–321.

Shulman, R.G., Hyder, F., Rothman, D.L., 2001. Lactate efflux and the neuroenergetic basis of brain function. NMR Biomed. 14 (7–8), 389–396.

Thompson, J.K., Peterson, M.R., Freeman, R.D., 2003. Single-neuron activity and tissue oxygenation in the cerebral cortex. Science 299 (5609), 1070–1072.

Valabregue, R., Aubert, A., Burger, J., Bittoun, J., Costalat, R., 2003. Relation between cerebral blood flow and metabolism explained by a model of oxygen exchange. J. Cereb. Blood Flow Metab. 23 (5), 536–545.

Vovenko, E., 1999. Distribution of oxygen tension on the surface of arterioles, capillaries and venules of brain cortex and in tissue in normoxia: an experimental study on rats. Pflugers Arch. 437 (4), 617–623.

Weiss, H.R., Buchweitz, E., Sinha, A.K., 1983. Effect of hypoxic-hypocapnia on cerebral regional oxygen consumption and supply. Microvasc. Res. 25 (2), 194–204.

Wu, D.M., Kawamura, H., Sakagami, K., Kobayashi, M., Puro, D.G., 2003. Cholinergic regulation of pericyte-containing retinal microvessels. Am. J. Physiol., Heart Circ. Physiol. 284, H2083–H2090.

Zheng, Y., Martindale, J., Johnston, D., Jones, M., Berwick, J., Mayhew, J., 2002. A model of the hemodynamic response and oxygen delivery to brain. Neuroimage 16 (3 Pt 1), 617–637.